AD-A171 703 ION CONDUCTING POLYMERS AS SOLID ELECTROLYTES(U) NAVAL 1/1
ACADEMY ANNAPOLIS MD J D SEMANCIK 28 MAY 86
USNA-TSPR-139

UNCLASSIFIED F/G 7/4 NL

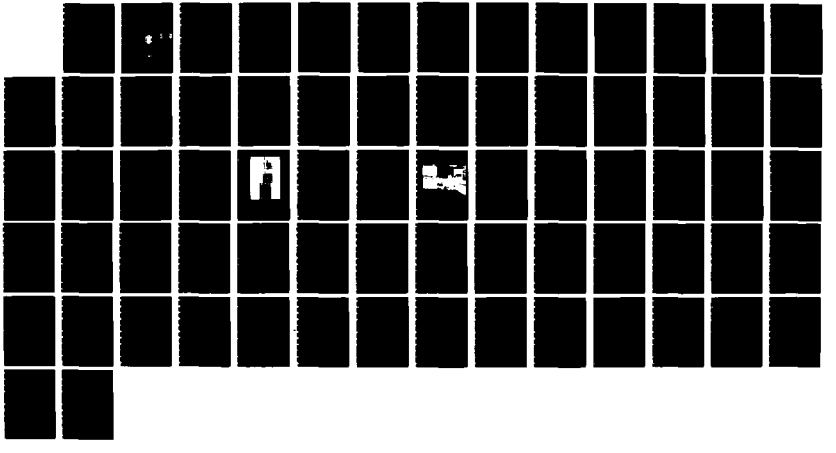

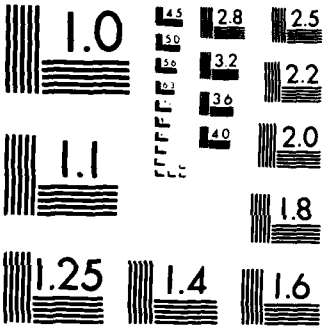

MICROCOPY RESOLUTION TEST CHART
NATIONAL BUREAU OF STANDARDS-1963-A

(17)

A TRIDENT SCHOLAR PROJECT REPORT

NO.
139

ION CONDUCTING POLYMERS AS SOLID ELECTROLYTES.

UNITED STATES NAVAL ACADEMY
ANNAPOLIS, MARYLAND

1986

UNCLASSIFIED

SECURITY CLASSIFICATION OF THIS PAGE (When Data Entered)

REPORT DOCUMENTATION PAGE		READ INSTRUCTIONS BEFORE COMPLETING FORM
1. REPORT NUMBER U.S.N.A. - TSPR; no. 139 (1986)	2. GOVT ACCESSION NO. ADA171703	3. RECIPIENT'S CATALOG NUMBER
4. TITLE (and Subtitle) ION CONDUCTING POLYMERS AS SOLID ELECTROLYTES.		5. TYPE OF REPORT & PERIOD COVERED Final: 1985/1986
		6. PERFORMING ORG. REPORT NUMBER
7. AUTHOR(s) Semancik, Jeffrey D.		8. CONTRACT OR GRANT NUMBER(s)
9. PERFORMING ORGANIZATION NAME AND ADDRESS United States Naval Academy, Annapolis.		10. PROGRAM ELEMENT, PROJECT, TASK AREA & WORK UNIT NUMBERS
11. CONTROLLING OFFICE NAME AND ADDRESS United States Naval Academy, Annapolis.		12. REPORT DATE 28 May 1986
		13. NUMBER OF PAGES 65
14. MONITORING AGENCY NAME & ADDRESS(if different from Controlling Office)		15. SECURITY CLASS. (of this report)
		15a. DECLASSIFICATION/DOWNGRADING SCHEDULE

16. DISTRIBUTION STATEMENT (of this Report)

This document has been approved for public release; its distribution is UNLIMITED.

17. DISTRIBUTION STATEMENT (of the abstract entered in Block 20, if different from Report)

This document has been approved for public release; its distribution is UNLIMITED.

18. SUPPLEMENTARY NOTES

Accepted gy the U.S. Trident Scholar Committee.

19. KEY WORDS (Continue on reverse side if necessary and identify by block number)

Polyelectrolytes
Electrolytes
Polymers and polymerization
Storage batteries
Submarines.

20. ABSTRACT (Continue on reverse side if necessary and identify by block number)

Electrically conducting polymers have recently been the subject of much interest. In particular, their potential as electrolytes in solid-state batteries has gained the attention of the U.S. Navy. Current ion-conducting polymers have conductivities which are too low by a factor of ten at operational temperatures. In order to be able to obtain suitable conductivities in these polymers, a thorough understanding of the mechanisms governing ion

(OVER)

DD FORM 1 JAN 73 1473 EDITION OF 1 NOV 65 IS OBSOLETE
S/N 0102-LF-014-6601

UNCLASSIFIED

SECURITY CLASSIFICATION OF THIS PAGE (When Data Entered)

motion in them must be attained.

The processes involved in the ion conduction of one particular polymer, poly(propylene oxide) or PPO, were studied in this research. Samples were prepared using an ion implantation procedure developed as part of the project as well as by the traditional chemical complexing technique involving alkali-metal salt doping. The samples produced were analyzed using both differential scanning calorimetry and audio frequency complex impedance measurements.

Results indicat that the polarity of the salts has a major effect upon the activation volume and the glass transition of PPO. As a result of the effects, it seems that non-polar anions may aid in increasing the cationic transport number of the ploymer. More importantly, the first direct numerical evidence of a connection between the large scale segmental motions of the polymer chains and the conductivity has been established.

U.S.N.A. - Trident Scholar project riport; no. 139 (1986)

"ION CONDUCTING POLYMERS AS SOLID ELECTROLYTES"

A Trident Scholar Report
by

Midshipman Jeffrey D. Semancik, Class of 1986

U.S. Naval Academy

Annapolis, Maryland

Mary C. Wintersgill

Advisor: Assis. Prof. Mary C. Wintersgill

Physics Department

Francis D. Correll

Advisor: Assoc. Prof. Francis D. Correll

Physics Department

Accepted for Trident Scholar Committee

Carl Schmidt

Chairman

28 May 1986

Date

Report Control Symbol USNA-1531-2

Electrically conducting polymers have recently been the subject of much interest. In particular, their potential as electrolytes in solid-state batteries has gained the attention of the U.S. Navy. Current ion-conducting polymers have conductivities which are too low by a factor of ten at operational temperatures. In order to be able to obtain suitable conductivities in these polymers, a thorough understanding of the mechanisms governing ion motion in them must be attained.

The processes involved in the ion conduction of one particular polymer, poly(propylene oxide) or PPO, were studied in this research. Samples were prepared using an ion implantation procedure developed as part of the project as well as by the traditional chemical complexing technique involving alkali-metal salt doping. The samples produced were analyzed using both differential scanning calorimetry and audio frequency complex impedance measurements.

Results indicate that the polarity of the salts has a major effect upon the activation volume and the glass transition of PPO. As a result of these effects, it seems that non-polar anions may aid in increasing the cationic transport number of the polymer. More importantly, the first direct numerical evidence of a connection between the large scale segmental motions of the polymer chains and the conductivity has been established.

ACKNOWLEDGEMENTS

A list of everyone who has made this project a success would be impossible to bring to mind at any one time. I would just like to mention those generous people who dedicated so much of their time, resources, and energies to see this research to its productive conclusions.

I would first like to express my thanks to LT Michael Smith whose help in the computer analysis of the data allowed so much of it to be looked in the span of just two semesters. Also, Charlie Holloway in the physics machine shop worked a lot of magic with the metal parts which made the ion implantation of samples possible, and he rightly deserves all the credit due him. I extend further thanks, and much of it, to Professor John Fontanella for his aid which he gave in so many areas and at so many times. Most of all, however, I must express my most sincere appreciation to my two advisors: Associate Professor Mary Wintersgill, who helped explain the alien field of polymers so that even I could understand it, and; Associate Professor Francis D. Correll, only he knows the time and effort we spent with his machine beneath Michelson Hall.

Thank You All;

You made it possible.

Jeffrey D. Semancik

Table of Contents

1. Introduction

The reactor on board the USS Baton Rouge (SSN 689) has just scrammed! The engineering watch quickly and efficiently executes an emergency shut down of the nuclear power plant and switches over to the emergency power reserve, a lead acid battery similar in many respects to that found in any automobile. As a result of the scram, the large and sudden power requirements placed on the battery and its subsequently high discharge, the meters in the control room are no longer an accurate indication of the battery's condition. A man, or more likely many of them, must be physically lowered into each of the 126 six-foot long cylindrical cells which comprise the ship's battery in order to measure the specific gravity and level of the water in them. A time consuming, to say the least, and potentially dangerous evolution.

Even on a good day, 4 of the 126 cells designated as pilot cells must be checked by sending personnel into them. Moreover, there are the possibilities of acid leakage and hydrogen (a very explosive gas) generation to contend with on a day-to-day basis; not the most welcome of circumstances in the environment of a submarine underway!

Then there are the matters of size and mass. Space and weight are two of the most vital parameters on a sub, and

the 126 cells take up a large portion of both. Besides, there is all of the associated equipment to consider, too: a special purification system to deionize the water used in the electrolytic solution and a bubbler to keep this solution moving to mention but a few.

One of America's most technologically advanced submarines is currently equipped with an emergency battery which is little more advanced than a Sears Die Hard! What the United States Navy really needs is a high energy density (for low weight and small size), easy care, non-volatile, and reliable battery.

Sounds impossible? Perhaps not! In recent years there have been scattered reports of all-plastic batteries meeting these specifications[1] . Unfortunately, none have yet been made which are operational below 100°C. The problem: the lack of a polymeric electrolyte[2] with suitable conductivities at low temperatures.

The research conducted for this work has aimed at gaining an insight into the mechanisms of the conduction of ions in polymers. It's direct goal has not been to produce

---

[1] "Battery Gets A Soft Cell", Sunday Times, London, 11-12-83.

[2] That portion of a battery which completes the circuit internally and accompanies the flow of current by the movement of ions towards the electrodes where they enter into the oxidation\reduction reactions taking place there.

a polymeric electrolyte suitable for use in a battery, yet it is a step in that direction. These two products are not unrelated, for once an understanding of the processes being dealt with has been attained, then this information can be applied towards the development of the desired electrolyte.

2. Conduction Theory

The measure of a material's ability to transport charge is known as its conductivity. Generally speaking, the higher the conductivity, the more charge is transported by the substance. The normal metallic conduction mechanism is the movement of electrons within a substance. However, many materials are capable of effecting conduction through the transport of ions introduced into them.

Historically, ion conducting substances have been liquids. The migration of the ions in these has been well studied. The discovery that certain polymers could also support sizeable ionic conduction currents has provoked much interest in the mechanisms involved in non-liquids.

2.1 Ion Conduction. For those materials which conduct ions, many factors affect the degree and effectiveness of the mechanism. Perhaps the most obvious and important of these is the structure, both physical and chemical, of the host substance. The material must be able to support the ions within its structure without restricting their motion nor chemically reacting with them. In fact, a good ion conductor will actually enhance the movement of the ions within it.

The characteristics of the ions themselves are also

determining factors in their migration. In particular, the number in which they are present and their mobility within the host material have a strong influence on the conductivity. The mobility of the ions, in turn, is dependent upon such considerations as their size and dipole moment. A dipole moment in an ion is a charge imbalance due to differing attractions for the electrons by the constituent atoms. The result is one end of the ion being more negative than the other. Often, an ion with a strong dipole moment will be electrically attracted to host molecules with local charge concentrations, thereby reducing its mobility considerably.

Within the host material, an ion is drawn to its energetically most favorable location, i.e. that of the lowest potential energy. The area surrounding the ion's location may also have energetically favorable centers. However, a certain energy "boost" is required to dissociate the ion from its current location and move it to the next site. The amount of energy in this "boost" is known as the activation energy, E_a, of the transport mechanism.

If there is a restoring force of some sort accompanying it, the movement of an ion is a resonance. The original situation is reestablished, or at least attempted to be, following a resonance. A free motion with no force tending to reestablish the previous positioning is known as a

relaxation. After a relaxation, the new arrangement remains until another boost is acquired. The conduction motion of ions is best described as a series relaxations.

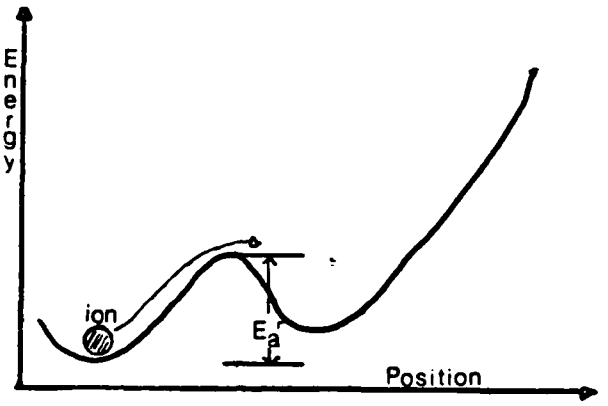

Figure 2.1
The ion's location in one dimension is along the abscissa and the potential energy as a function of position is the ordinate. An ion must possess at least energy E_a in order to move from its current position to the adjacent one.

Another parameter of significance in the study of ion conductivity in polymers is the activation volume. As with the activation energy, the activation volume is associated with an ion moving from one favorable location to another. More specifically, it represents the amount of expansion necessary to allow an ion to migrate.

The conductivity of an ion containing material is typically attributed to both positively and negatively charged species. In many applications, the mobility of one species and the suppression of the other is desired. A measure of the percentage of the conduction current carried by each is known as the transport number of the ion. Unlike

many of the other factors, the transport number is difficult to determine precisely and is, thus, often a subject of debate.

2.2 Measurement. The conductivity, σ, is directly related to the bulk resistance, R_b, of a material by a simple geometric factor:

$$\sigma = L/R_b A$$

where L is the length and A is the cross-sectional area of the conduction path. This simple relationship makes the conductivity an easily measured quantity for a sample of known geometry, requiring only that the bulk resistance be found.

The bulk resistance is the opposition to the flow of electricity when the imaginary component of the complex impedance goes to zero. Although it can be measured in a simple d.c. circuit, a much more accurate method which also reveals information on the ion transfer mechanism has been developed by W. Archer and R. Armstrong[3] through the use of a.c. complex impedance measurements.

When a sinusoidal time-dependent voltage of the form

$$e=E \sin(wt)$$

---

[3] W. Archer & R. Armstrong, Electrochemistry, 7, 157 (1980

where $w=2\pi f$ is the angular frequency is applied across a conducting sample, a sinusoidal current

$$i=I \sin(wt+\delta)$$

flows. Current also flows for frequencies $w=2w,3w,\ldots$ Here is the phase difference between the applied voltage and the resulting current. By taking the ratio of the two, a vector quantity, Z, the impedance, can defined such that its magnitude is the ratio:

$$Z=E/I$$

and the angle is:

$$\theta_z=-\delta.$$

Projected onto a complex plane the impedance can be expressed in polar form with real and imaginary parts

$$Z=Z'+jZ''.$$

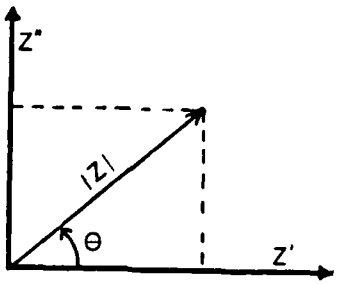

Figure 2.2

Replacing the sample with a pure resistance of magnitude R yields

$Z=R$ and $\theta_z=0$.

Similarly, a purely capacitive sample with capacitance[4] C gives

$Z=1/wC$ and $\theta_z=90^o$

Different combinations of resistances and capacitances will likewise lead to unique complex impedance graphs. By matching the graph of the sample's impedance to the appropriate circuit's, a model for the sample is obtained. The significance of the various components in the equivalent circuit can then be interpreted as specific physical mechanisms in the conduction process. The point of intersection with the real axis gives the value of the bulk resistance for the circuit.

As an example, a capacitance and a resistance in parallel produce an impedance plot in the form of a semicircle (see figure 2.3). If this was the plot for a sample, the capacitive portion would be associated with the geometric

---

[4] Capacitance is a measure of the ability of a material to store charge and is given by C=QV.

capacitance of the sample and the resistance with the bulk value.

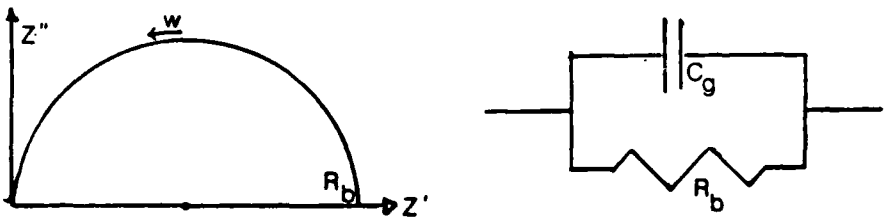

Figure 2.3 The bulk resistance is Rb.

3. Polymers

Polymers, more commonly recognized as plastics and rubbers, are organic materials which are composed of chains of chemical units, known as monomers. These monomers are molecules in their own right. Through the process of polymerization, they react together chemically to form the polymer chain. The bonding which holds the monomer units together is quite strong along the chains, yet only a relatively weak attraction exists between the individual chains. As a result, these "macromolecules" offer many unique and useful properties depending on the monomers they are composed of and the size of the chains formed. Among the favorable qualities are their ease of fabrication and relative cheapness.

3.1 Classification. Polymers can be divided into three major classes: thermosets (epoxies); rubbers, and; thermoplastics (or simply plastics). Thermoplastics can further be separated as crystalline, having a regular lattice structure, or amorphous, oriented and arranged at random.

The polymers which have been reported to exhibit some ion conductivity have all been thermoplastics. Although some of them are crystalline under normal circumstances, their ion conductivity seems to restricted to their amorphous condi-

tion. Poly(ethylene oxide), PEO, is the best known material in this group.

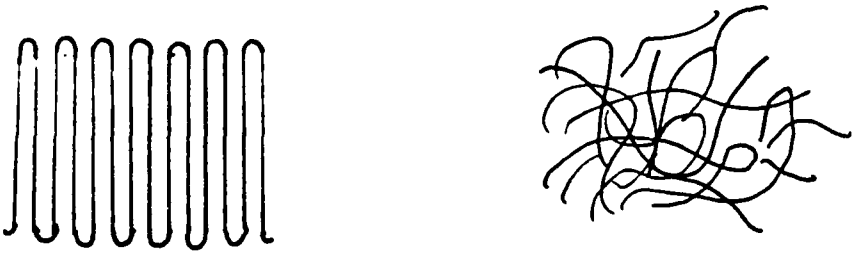

(a) crystalline (b) amorphous

Figure 3.1. Thermoplastic structure.

3.2 The Glass Transition. Amorphous polymers are, for this reason, the obvious choice for the study of ion conduction. These materials are best characterized by the glass transition associated with the α relaxation. This transition is the progression of the polymer from a glass-like to a rubber-like state, and the α relaxation is related to the increasing motion of the polymer chains. This transformation occurs at and is characterized by a temperature, T_g. Actually, the glass transition occurs over a 10° to 40° C range. This very fact distinguishes it from the so-called first order transitions such as melting and vaporization which take place discontinuously at a specific temperature. T_g is, therefore, usually defined as the onset temperature, although middle and end temperatures can also be used, of

the glass transition where the rate of change of various properties, such as the coefficient of thermal expansion, with respect to temperature begins to vary. It may also be referred to the central or end temperature of the region, and proper specification is thus required. The physical properties of the polymer above and below the glass transition are quite different. For instance, above Tg the chains, which are effectively "frozen" out in the glassy material, are free to rotate and translate.

One approach toward understanding the glass transition is the free volume model. Free volume is the "empty space" not occupied by the actual polymer chain. According to this model, when the polymer is in the rubber region the free volume is quite large and the chains are relatively free to move around. The amount of free volume is directly related to temperature, a lowering of which correspondingly reduces the open space. When the free volume is diminished enough that free rotation and translation of the chains is no longer possible, the material enters the glass region.

D. Shriver, B. Papke and M. Ratner have outlined another theory, proposed by Gibbs and coworkers,[5] describing the behavior of amorphous polymers under going the glass transition which is concerned with the configurational

---

[5] B. Papke, M. Ratner, and D. Shriver, J. Electrochem. Soc., 192, 1694 (1982).

entropy of the material. The configurational entropy is related to the number of possible arrangements of the polymer chains. In the rubber state, this entropy is directly related to the temperature, decreasing proportionally as Tg is approached from above. As the glass transition is completed, the configurational ground state is reached. That is, the polymer is in its most favorable arrangement, that of lowest energy, in which it will remain throughout its glass state regardless of temperature. Once the polymer is in this ground state, no further entropy is lost to motion of the chains.

3.3 Poly(propylene oxide). The polymer studied in this research was poly(propylene oxide), more commonly referred to as PPO. It is a highly amorphous material exhibiting no crystallinity. The repeating monomer unit is:

$$[-CH_2-CHCH_3-O-]_n .$$

The molecular weight of the chains is on the order of 3000 grams/mole.

The presence of the oxygen atom in the monomer offers sites of higher electron affinity in the chains. That is to say, the electrons of the polymer are more strongly attracted to the oxygen atoms and, thus, tend to spend more time

in their vicinity. This tends to create localized regions of charge along the chains.

The presence of these charged areas along the PPO chains gives them the ability to dissolve certain salts. This is accomplished by the dissociation of the ionically bound salt molecule into its positive and negative constituents. With this capacity to hold ions in solution, PPO becomes a very good candidate for their transport.

4. The Experiment

4.1a Sample Preparation (Salt-Complexed). The material properties of polymers makes them rather well suited for use in the construction of batteries. These same characteristics also aided in the fabrication of samples for use in this research.

Parel elastomer was purchased from Hercules, Inc. in block form. The testing apparatus to be used required that the samples be thin enough (approximately 1mm) to fit between the electrodes of the holder and also to provide good electrical contact with it. Moreover, since the host material does not contain any of its own, the ions had to be introduced, with some degree of uniformity, into the polymer. The nature of the material allowed both of these specifications to be met without much difficulty.

From the block of PPO a number of smaller pieces (totalling 5 to 6 grams) were cut. These were then dissolved in a jar of methanol and left overnight with a magnetic stirrer turning it to form a highly viscous solution.

The choice of salts to be used as dopants favored the use of lithium salts. One of the reasons for the preference was that the alkali metal salts dissociate the most easily and completely due to their low affinity for their outermost electron. The lithium ion is the smallest of the alkali

metals, and its mobility is thereby less constricted within the polymer. Another important reason for the choice of lithium salts is that current electrode technology favors the use of lithium due to its high electronegativity which makes it capable of producing a large potential step. Unfortunately, it also reacts violently with water, the solvent of liquid electrolytes.

The salts were also chosen on the basis of their anion. In particular, an effort was made to include anions of different dipole moments and sizes. Table 4.1 lists the salts used to dope the PPO and relates some information on their anions.

Table 4.1

Anion Name	Formula	Radius	Dipole Moment
Triflate	CF_3SO_3-	(largest)	yes
Perchlorate	ClO_4-	2.45 Å	no
Thiocyanate	SCN-	2.20 Å	yes
Iodide	I-	2.10 Å	no

The salt was added to the methanol-PPO solution in a predetermined proportion by mole fraction and allowed to dissolve completely at room temperature. As all of the salts used were extremely hygroscopic, care had to be taken to insure that no water entered into the samples. For this

reason, the salts were first dried in a vacuum oven at 75° C for 24 hours. In addition, all further preparation of the samples took place within a dry box in flowing nitrogen or dry air. Relative humidity within the dry box was kept below 10% at all times.

Once well mixed, the samples were poured into glass rings onto teflon sheets. As a rule, two casting were done: the first to seal the ring to the teflon and the second to achieve the desired sample thickness. The molds were allowed to dry at room temperature. The samples were then removed from the dry box and dried further in a vacuum oven at 65° C overnight.

When the various samples were examined after drying, cloudy and clear regions were observed in some of the castings. Upon closer scrutiny it was discovered that these regions appeared in those samples where the salt doping concentration was less than one part in eight [proportions varied from 4:1 up to 24:1 (PPO:salt)]. It was concluded that this 8:1 ratio was favored by the complexed PPO. It was hypothesized that in the cloudy regions the salt had migrated so that the local doping was 8:1. If this were the case, the rest of casting would be pure PPO. Since thorough mixing seemed to favor the 8:1 ratio of PPO to salt, the rest of the samples were prepared in this same proportion.

Finally, a means of maintaining good electrical contact

between the polymer sample and the contacts of the test equipment was accomplished by evaporating aluminum onto the surfaces of the PPO casts in a vacuum. One side was completely coated while the other was masked so as to produce a number of aluminum circles. Cutting these out yielded the final samples approximately 1mm thick and 15mm in diameter.

4.1b Sample Preparation (Ion Implanted). The method of preparing the samples with various salts introduced not only the positively charged cations but also the negatively charged anions into the polymer. Since a good electrolyte conducts primarily by cation motion, an alternate method of preparing the samples so that only the positive ions are introduced was sought. Ion implantation offered a manner of doping the polymer with just one charged species.

Ion implantation uses a low-energy ion accelerator to propel fast ions into the near-surface region of the host material. The ion implantation facility at USNA consists of two major components: a small (400 kV) Van de Graaff generator and an extended beamline.

The Van de Graaff accelerator is the source of the fast ions. The Academy obtained its accelerator as surplus property from the Naval Surface Weapons Center, White Oak. Slow ions are produced inside the accelerator, in a device

known as an ion source; different types of ion sources may be used to provide different kinds of ions. The ions are extracted from the source by a specially shaped and biased electrode, and are introduced into an evacuated accelerating tube, where a strong electric field produced by the Van de Graaff generator focuses and accelerates them to a few percent of the speed of light before they emerge from the accelerator in the form of a beam.

Because the ions emerging from the accelerator at any time may be of several different types and charges depending upon the conditions in the ion source, it is necessary to carefully select the ones to be implanted into the material. For this purpose, a six-inch momentum analyzing magnet was employed. The principle of magnetic analysis is based on the fact that an ion passing through a magnetic field will be deflected by a force that is proportional to its speed and the strength of the field. As a result, a singly-charged particle moving at right angles to a uniform magnetic field will follow a circular path whose radius r is given by

$$r = pc / 300\ B$$

where pc is the momentum of the particle in electron volts (eV), B is the magnetic field strength in Gauss (G), and the

radius r is expressed in centimeters (cm).

In order to enter the beamline and eventually strike the sample, the desired ions were made to bend through an angle of 25° as they passed through the analyzing magnet. The momentum, and therefore the energy, of such ions can be determined from the known geometry of the magnet and the measured magnetic field. If the field is assumed to be uniform over a rectangular area of length l, as shown in figure 4.1. the momentum of the ions deflected through the required 25° angle can be determined from the equation

$$pc = 300\ Bl/\sin 25^\circ$$

If the mass m of the ions is also known, then their kinetic energy Ek may be obtained from the nonrelativistic expression

$$Ek = (pc)^2/2\ mc^2$$

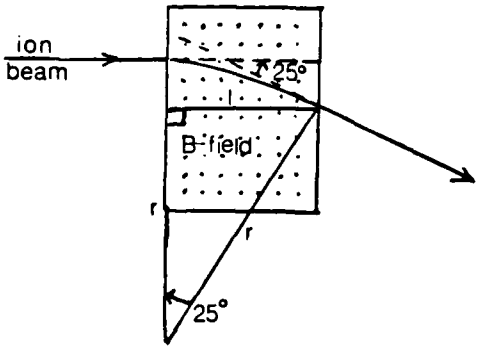

Figure 4.1

After leaving the analyzing magnet, the ion beam enters

the extended beamline and passes through two orthogonal sets of parallel-plate scanning electrodes. Applying different voltages to the plates in each set produces an electric field between the plates; one set of plates produces a horizontal field, while the other produces a vertical field. These fields can be used to steer or sweep the ion beam in a raster pattern (as in a television tube) so that it covers the sample uniformly.

Finally, the beam enters the implantation chamber where it strikes the polymer sample. The sample is supported by a special holder, shown in figure 4.2. This holder, which was designed and constructed at USNA specifically for this project, allows two samples to be implanted without opening the vacuum chamber, and permits careful monitoring of the dose delivered to each implanted sample.

In the sample holder, the polymer film (prepared in the same manner as the salt complexed samples except that no salt was added prior to drying) is held onto a thick block of aluminum by tantalum frame. The raster-scanned ion beam strikes the tantalum frame and polymer sample; a portion of the beam also passes through three carefully placed holes of known diameter drilled through the frame and aluminum block. The beam that passes through these holes then strikes a tantalum backing sheet which is electrically insulated from the aluminum plate, and the charge it deposits is collected

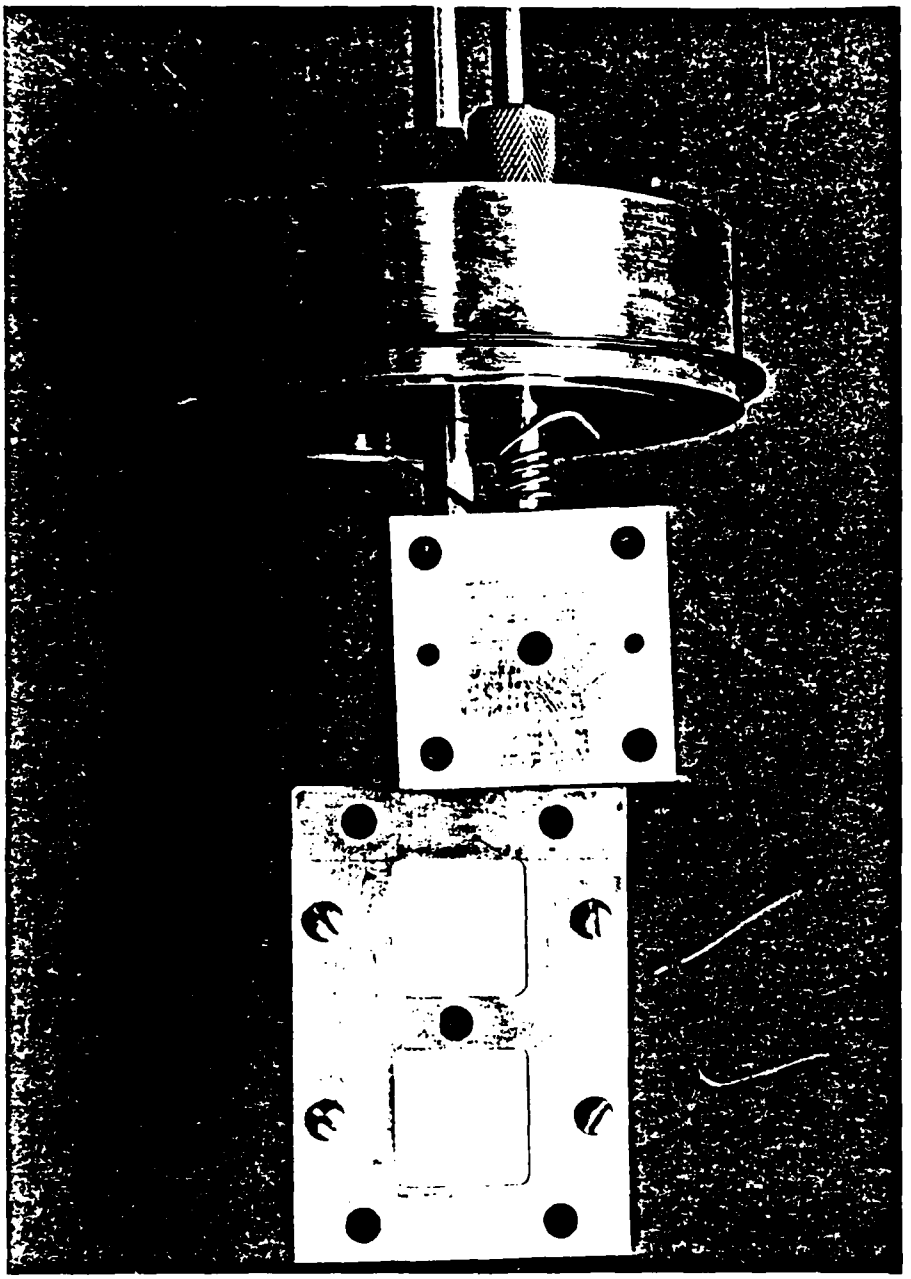

Figure 4.2 Ion implantation sample holder.

and conducted to a device known as a current integrator (Ortec model 439). The current integrator produces a standard electrical pulse for every 10^{-10} Coulombs of charge (or 6.25×10^{8} singly-charged ions) collected. These pulses are counted in a scaler (Ortec 482) to determine the total number of ions per unit area passing through the holes. If the beam is uniformly swept over the sample and surrounding frame, then this number is also equal to the number of ions per unit area (or dose) implanted in the polymer. Once the required dose is reached, a beam-stopping shutter is lowered in front of the sample.

The holes in the sample holder also provide a method of insuring the entire sample area is covered by the scanned beam. The scanning signal is used to drive the X-Y inputs of an oscilloscope, while the output pulses of the current integrator are stretched and applied to the Z input to intensify the oscilloscope trace. The result is a series of short, bright lines on the oscilloscope screen whenever the beam passes through one of the holes in the sample holder and is collected by the current integrator. Since the holes surround the sample in a triangular pattern, observing images of all three holes on the oscilloscope insures that the beam is scanned over the entire sample.

A photograph of the extended beamline is shown in figure 4.3. This beamline was completely designed and constructed

as part of this project, using a variety of existing, specially-built, and newly purchased parts. The implantation chamber and nearby components are made entirely of stainless steel and aluminum.

The extended beamline and the accelerating tube inside the Van de Graaff must be maintained under vacuum to prevent the unwanted collisions of the ion beam with residual gas molecules. Two high-vacuum pumps (a cryogenic pump near the implantation chamber and a diffusion pump near the accelerator) were used for this purpose. Beamline pressures were kept at or below 2×10^{-6} torr, except for a short period whenever the ion beam first hit the new polymer sample. At those times, the pressure rose briefly to around 5×10^{-5} torr, apparently because the fast ions heated the polymer and caused water vapor and the more volatile components of the polymer to be released (or "outgassed"). This hypothesis was generally confirmed by the use of a residual gas analyzer (Dycor Electronics model M100) attached to the beamline near the implantation chamber. This device uses a radio-frequency mass spectrometer to measure the partial pressures of the various gases present in the vacuum system, and it presents the results as a function of the molecular mass. During the first moments of ion beam bombardment of a fresh sample, the partial pressures of water vapor and of

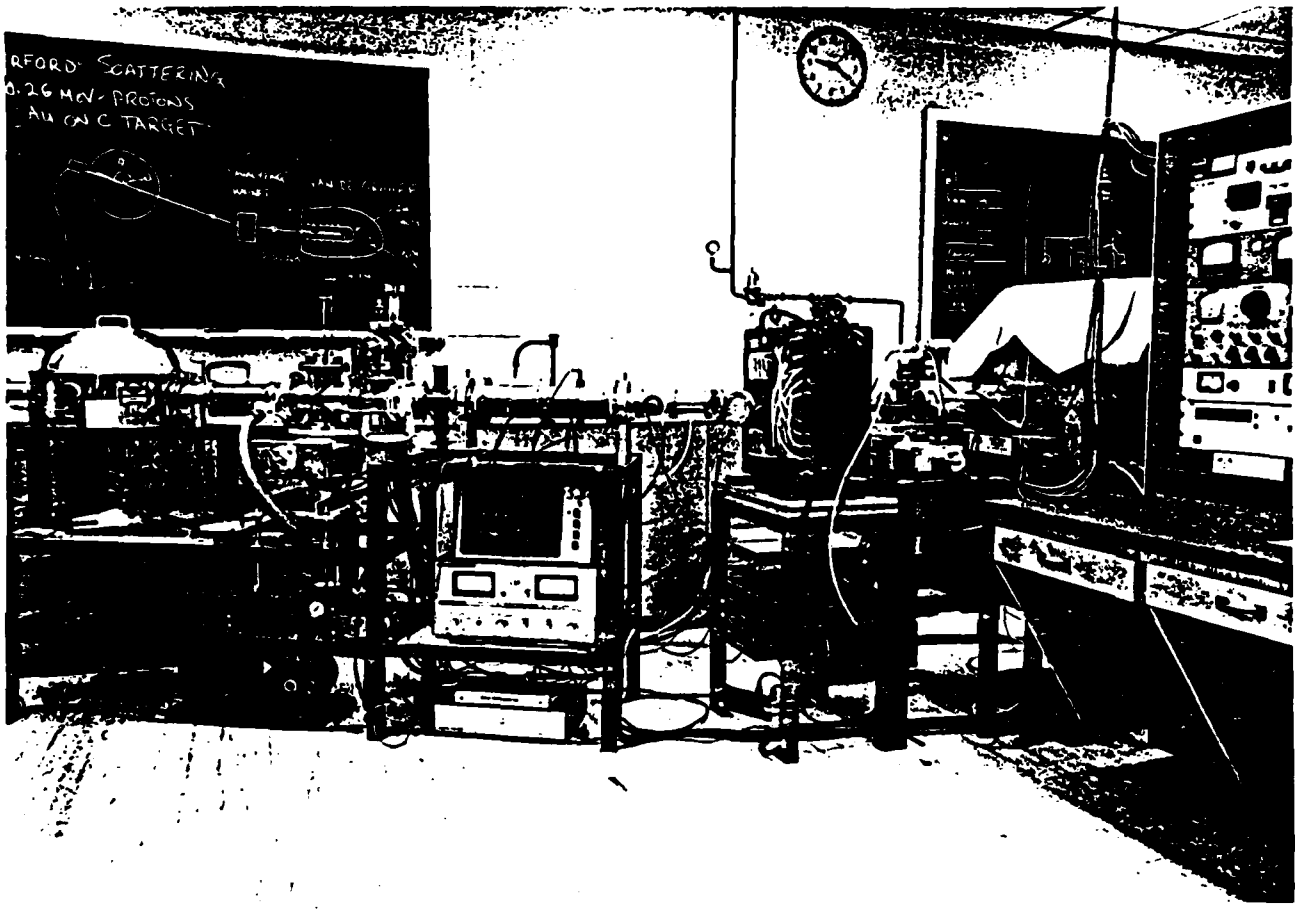

Figure 4.3 The extended beamline.

several high-mass molecules rose dramatically, and then dropped to nearly the original low levels. Although it would require careful study to verify that the molecular masses detected were actually those expected from bombardment of the polymers used, this seems to be a reasonable assumption consistent with the observations.

Three implantation were performed using hydrogen ions either H^+ ions (protons) or H_2^+ ions (singly-charged hydrogen molecules which presumably break up immediately upon impact with the polymers). Hydrogen ions were chosen in part because of their easy availability and convenience for testing the system, and in part because they could be used to investigate damage to the polymers caused by the implantation. The ion source used for the hydrogen implantation is of the common radio-frequency type; it consists of a pyrex bottle into which hydrogen gas is admitted by an electrically-controlled valve and ionized by the application of a strong, radio-frequency oscillating electric field. The resulting positive ions (H^+ or H_2^+) are repelled from the source bottle and into the accelerating tube by applying a positive potential to a special electrode. Hydrogen ion currents on the order of tens of microamperes are routinely obtainable. This kind of source can also be used to produce ions from other gaseous elements or compounds, such as He or CO_2; success obtained during this project with the H ions

demonstrates that further developments needed to produce and accelerate these heavier ions should be relatively simple.

Although the radio-frequency source is convenient for producing many different kinds of ions, it cannot easily produce large currents of alkali metal ions, such as the lithium ions needed for the remainder of this study. For this purpose, a special alkali-metal source was purchased (Phrasor Scientific, Inc.). This particular kind of source produces positive alkali ions by thermal emission from a pressed, alkali-aluminosilicate compound, and currents on the order of tens of microamperes are claimed to be available. These relatively high currents, together the low cost and modest power requirements of this kind of source, seem to make it an attractive one for use in small Van de Graaff accelerators, although it seems that no one has attempted to use this way prior to this project.

Adapting the source for use in the accelerator, although apparently a straightforward procedure, was more time consuming than expected, and has still not been completed. Delays were experienced in machining and testing some of the needed adapters, which required vacuum-tight soldering of several stainless steel pieces (an often difficult task) and in constructing special electronic circuits to monitor the operation of the source while it is in the accelerator and at a voltage of about 250,000 volts with respect to ground.

When it became apparent that the lithium source development would not be completed as soon as expected, it was decided to use the lithium source without the Van de Graaff to implant very-low-energy ions into at least one polymer sample. The lithium source and a polymer sample mounted in a very simple holder were placed in a vacuum of about 1 x 10^{-6} torr, facing one another and separated by about 20 cm. The lithium source was operated just as it would be in the Van de Graaff accelerator, but a small d.c. power supply was used to provide an accelerating voltage of about 800 volts. A beam current of about ten microamperes was obtained, and the lithium ions were implanted into the sample without focusing or scanning.

The conditions of the various implantation are summarized below.

Table 4.2

Projectile	Energy (keV)	Velocity (km/sec)	Dose (10^{15}/cm^2)	Mean Depth[6] (micrometers)
H_2^+	188	4300	2.5	2.0
H^+	181	5900	5	3.2
H^+	230	6600	5	3.7
Li^+	0.8	150	5	< 0.1 [7]

[6] Depths from L.C. Northcliffe and R.E.Schilling, Nuclear Data Tables, A7, 233 (1970).

[7] This is a rough estimate as tables for energies this low were not available.

4.2 Differential Scanning Calorimetry. Differential scanning calorimetry, DSC, is type of thermal analysis measuring of changes in a physical property as a function of temperature. In a thermal analysis system a sample is placed in a carefully temperature regulated environment. The changes in the physical properties are detected by an appropriate transducer, amplified, and recorded on some sort of output device, usually an X-Y recorder. Different analysis techniques employ transducers specifically suited for the measurements being made. The rest of this so-called "generic" system is common to all forms of thermal analysis. A schematic of the generic system is shown in figure 4.5

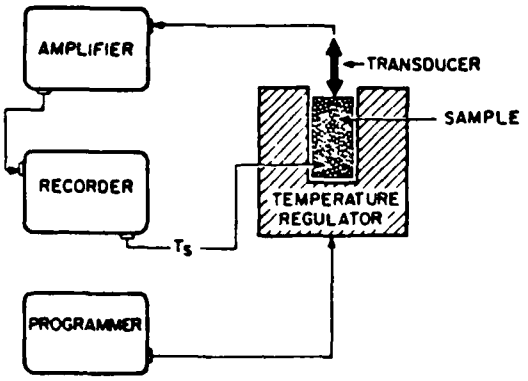

Figure 4.5 A modern thermal analysis system (Paul F.Levy in "Thermal Analysis: An Overview", American Laboratory, January 1970)

In DSC the physical parameter measured is the amount of heat transferred into a sample. The transducer used is a

thermocouple connected between the sample and a reference pan. In order to maintain a well controlled heat path to the sample and reference and to provide an external connection from the sensor to the sample, both are placed on a thermoelectric disk of carefully designed dimension and configuration. A thermocouple between the sample and reference is realized by attaching two wires (electrically complimentary to the disk material) to them. Because the thermal resistances to both are constant, any differential in temperature is directly proportional to the differential heat flow. A third wire is also connected to the sample to provide a signal proportional to its temperature. By plotting the differential heat flow response versus the temperature signal from the sample, the X-Y recorder

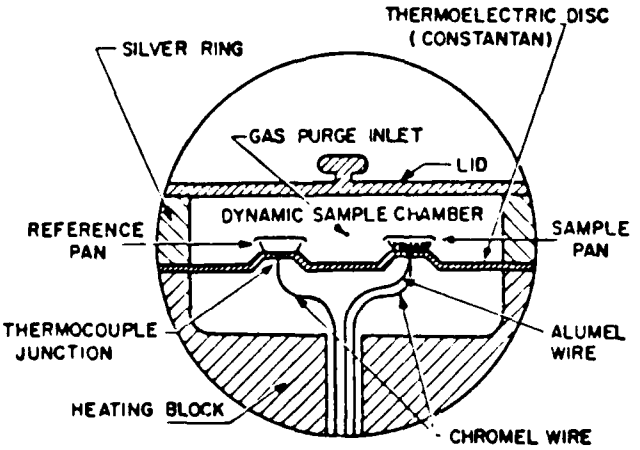

Figure 4.6 A DSC cell cross section (Paul Levy in "Thermal Analysis: An Overview", American Laboratory, January 1970)

produces an output curve, the area under which is directly

proportional to the amount of heat transferred into or out of the sample.

Of particular importance on the DSC plot is the glass transition. It is marked by a characteristic endotherm rather than the endo/exotherm "dip" associated with melting.

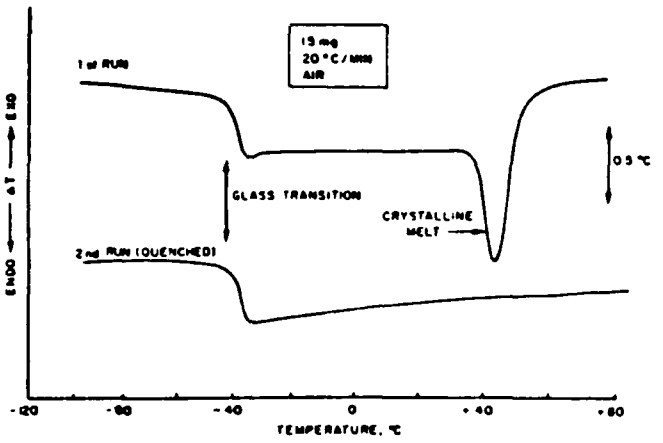

Figure 4.7 Characteristic thermograms (Paul Levy in "Thermal Analysis: An Overview", American Laboratory, January 1970)

The instrument used in this research was the DuPont 910 DSC cell used in conjunction with the Dupont 990 Thermal Analyzer. Values for the onset, middle, and end glass transition temperatures were taken for all of the samples.

4.3 Complex Impedance Measurements. The benefits of complex impedance analysis are only available to the extent that precise impedances can be measured. A fully automated CGA-82 microprocessor-controlled impedance bridge provided the

accuracy required.

The principle of operation of the complex impedance bridge is very similar to that of the more familiar Wheatstone bridge except that impedances are substituted for the simple resistances and the supply voltage is varied along with a resistor. A sample of unknown resistance, R_s, and capacitance, C_s, is placed across a known voltage, V_1. Balanced against this is a constant capacitance, C_k, and a variable yet known resistance, R, and voltage, V_2, (varied through a transformer). When the current through the detector is zero:

$$i_s = i$$

For this to hold:

$$V_1 = i_s R_s = i_s / (wC_s)$$

$$V_2 = iR = i/(wC_k)$$

Combining these yields the following equations for the capacitance and the conductance, $G_s = 1/R_s$, of the sample:

$$C_s = V_1 C_k / V_2$$

and

$$G = RV_1 / V_2$$

The bridge used found the values for C_s and G_s/w for seventeen frequencies from 10 Hz to 100 kHz. The figures

were recorded simultaneously on an Apple-IIe computer which provided the microprocessor control.

The samples were tested over a range of both temperatures and pressures. The apparatus used for both was the same and consisted of a high pressure bomb containing the samples immersed in a temperature bath. Within the pressure bomb two separate samples were analyzed by the complex impedance bridge over the full range of frequencies. Each was held by spring loaded electrodes from which leads to the bridge were attached.

A simplified diagram of the impedance bridge is shown in figure 4.8.

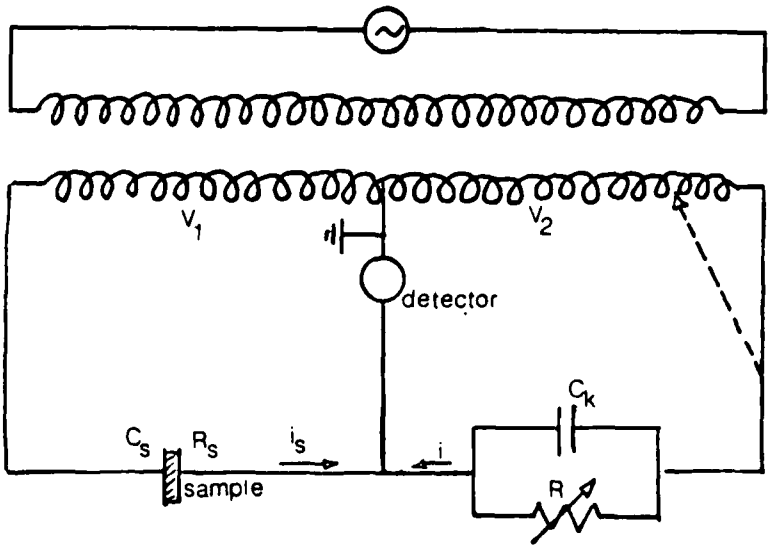

Figure 4.8 Schematic of a complex impedance bridge (G.C. Kolodziejczak in Radiation Induced Dielectric Relaxation In Rare Earth Doped Calcium Fluoride. Report to the Trident Scholar Committee. Annapolis, MD: U.S. Naval Academy, 1978)

The pressure in the bomb was maintained by hydraulic fluid. Two different high pressure liquids, Spinesstic 22 (Exxon) and Fluorinert FC-77 electronic liquid (3M Co.), were used in order to detect any possible reaction of the samples with the fluid. The polymers were brought to the desired pressure by a low pressure hydraulic pump operating through an intensifier and a high pressure hydraulic pump connected above the intensifier when necessary. The pumping was the only task in the experiment that had to be done manually once the apparatus had been set up. The pressure was applied directly to the samples.

The temperature of the bomb was maintained by a large temperature bath of oil. A thermostat controlled a series of heater coils, turning them off and on as necessary in order to keep the temperature to within a tenth of a degree (Celsius) of the set value. Stirrers ensured that the heat was distributed through the oil uniformly.

Complex impedance measurements were taken in two types of runs: isothermal and isobaric. When conducting the isobaric runs, varying the temperature at a constant pressure, thirty minutes were necessary to allow for the changes in the temperature to be realized within at the sample. This was the result of the indirect heating method used as the temperature first had to be obtained in the bath fluid and then transmitted through the thick walls of the pressure

bomb. In the isothermal runs the temperature was maintained constant as the pressure was varied. An equilibration time of twelve minutes was sufficient to allow any temperature fluctuations due to the pressure changes within the pressure bomb/sample holder to dampen out since the temperature of the bath and bomb did not vary significantly and the pressure was applied directly.

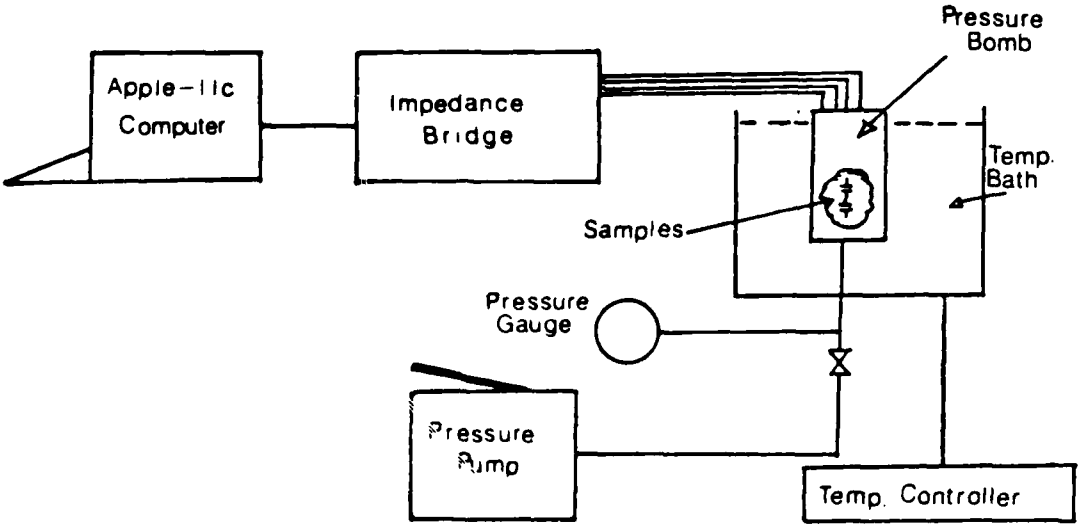

Figure 4.9 Apparatus for complex impedance measurements

5. Results

5.1 Differential Scanning Calorimetry. DSC measurements were carried out on pure PPO as well as that complexed with the four lithium salts. Each of the five samples exhibited only a glass transition. Since no dips in the thermograms characteristic of crystalline melting were observed, this indicates that all were completely amorphous in nature. Values for the onset, middle, and end temperatures are given in table I. It is obvious that the introduction of the salts into the polymer shifts the temperature of the glass transition upwards by a significant amount.

Quenching, heating followed by a rapid cooling, was tried with the samples. The thermogram in figure 5.1 shows its effects upon the glass transition. As the transition becomes sharper, the onset and end temperatures shift. The middle temperature, however, remains constant, indicating it is the most accurate measure of Tg.

5.2 Complex Impedance. The data obtained from the complex impedance bridge gave the conductance and the capacitance of a sample over a range of seventeen frequencies at set pressure and temperature. The bulk resistance of the sample was determined by complex impedance analysis as described above.

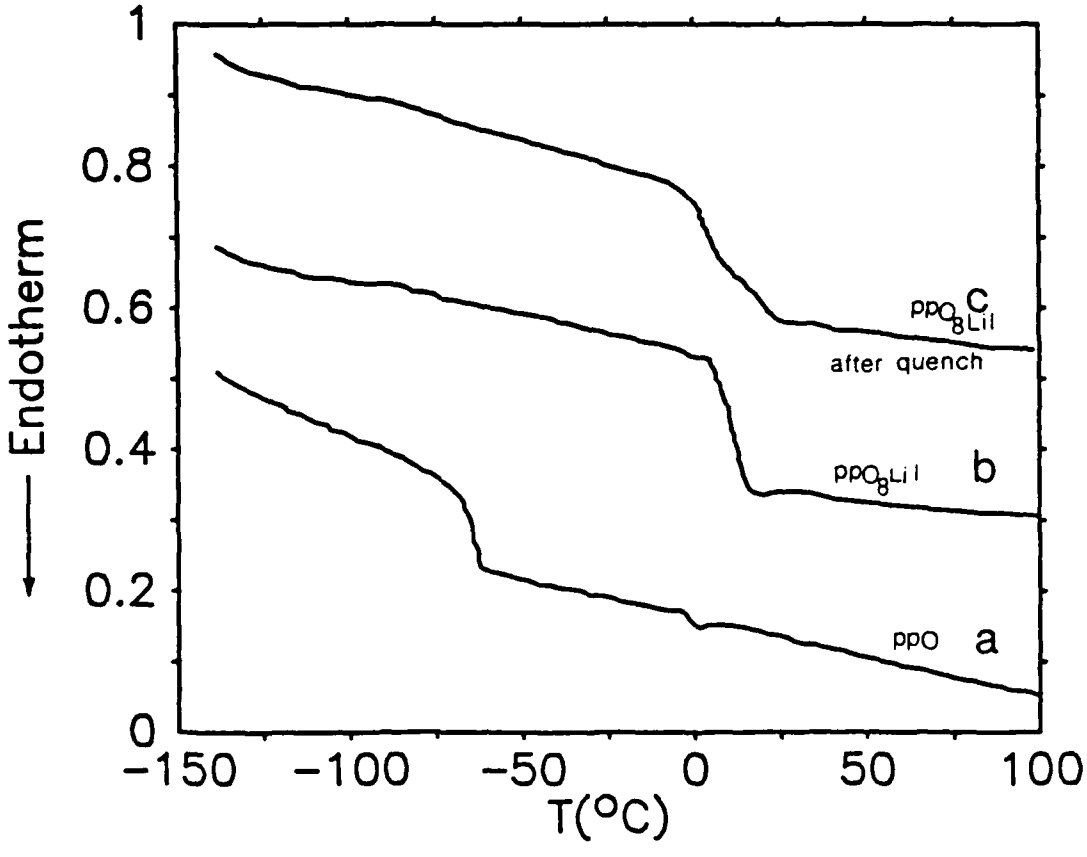

Figure 5.1 Thermograms of salt-complexed PPO.

A typical complex impedance plot is shown in figure 5.2. Two distinct segments can be seen: a semicircle and a straight line. The straight line is characteristic of a capacitance in series with a resistance, and the semicircle is indicative of a parallel combination of a resistance and a capacitance. It should be noted that the series capacitance dominates at the low frequencies while the high frequencies are governed by the parallel capacitance. All of the samples utilized exhibited similar behavior. The equivalent circuit for the samples is thus

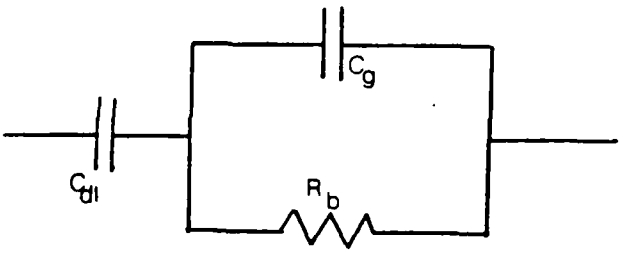

Figure 5.3

The components of the equivalent circuit represent real effects within the material. The resistance is the bulk resistance, R_b, of the sample. The capacitance in parallel with the it is the geometric capacitance of the polymer, C_g, which is due to its presence as a dielectric between the two contacts. The series capacitance is known as the double layer capacitance, C_{dl}. It is caused by the buildup of ions along the electrode-sample interface. Notice that this is

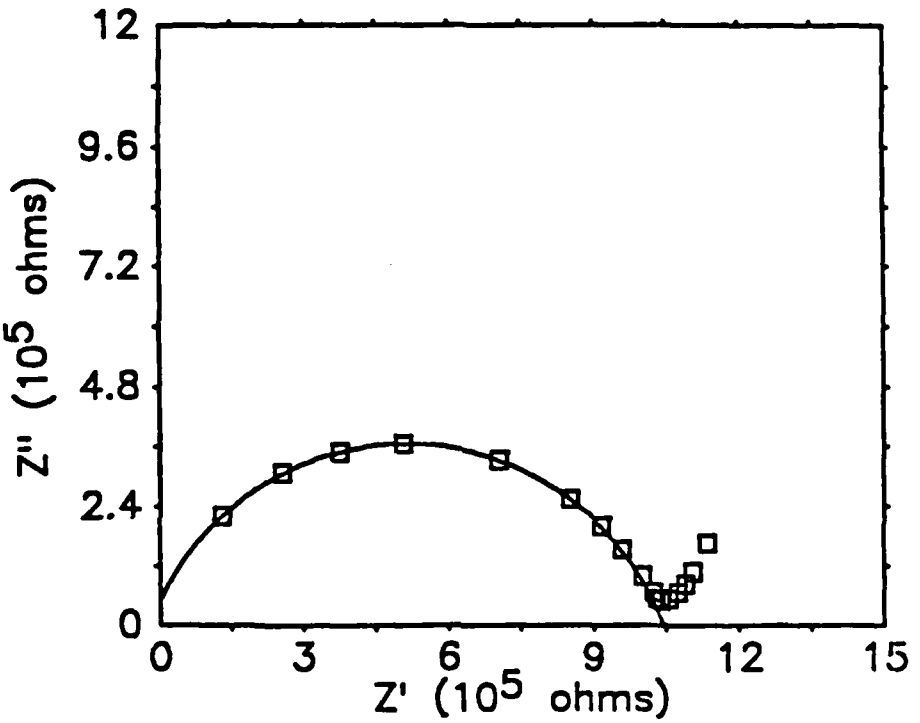

Figure 5.2 A typical complex impedance plot.

consistent with its dominance at low frequencies as higher frequencies prevent this buildup by reversing the polarity of the electric field before they can accumulate.

There is, obviously, a degree of deviation in the impedance plots of the samples from that of the idealized equivalent circuit. Archer and Armstrong address a number of possible causes for such differences in their presentation of complex impedance analysis.[8] The theoretical model used in the development of the technique is based on ideal electrodes in contact with a perfect material of high ionic conductivity. Thus, the deviations arise from physical variations from this model.

Perfect electrodes assume complete contact with the dielectric material. The surfaces of the polymers were not ideal. The roughness of the contact area results in the slope apparent in the straight line portion of the impedance plots of the polymers.

The circular segment of the plots is also distorted. In particular, it is flattened, pushing the intersection of the circle and the line segments upwards. This flattening is due to the conduction of ions in directions other than perpendicular to electrodes. This may be caused by a number of factors including the physical blocking of the direct

---

[8] W.I. Archer & R.D. Armstrong, Electrochemistry, 7 (1980) 198.

conduction path by the polymer chains of the host material.

The end result of these deviations is the complication of the extraction of the bulk resistance from the plots. The fitting of the depressed arc observed for the high frequency branch using a Cole-Cole distribution[9]:

$$Z^* = Z_o/[1+(iw\tau)^{1-\alpha}]$$

where Z_o, τ, and α are constant fitting parameters, results in values for the bulk resistance of the samples. As the temperature of measurement was increased less of the semicircle was apparent on the impedance plots and a combination of the depressed arc and the slanted vertical line was utilized to obtain the bulk resistances.

The amount of data taken by the complex impedance bridge was substantial, and the computer thus became an essential factor in its reduction. The results of the complex impedance measurements were originally stored on standard floppy disks as they were taken on an Apple-IIe computer. After a run was completed, the data was transferred to the Naval Academy Time Sharing System, NATS. Once on NATS, the data was subsequently reduced by a series of programs to obtain values for the conductivity as functions of temperature or pressure.

---

[9] M. Armand, Solid State Ionics, 9 & 10, 745 (1983).

5.3a Analysis: Conductivity. The base ten logarithms of the conductivities obtained from the isobaric runs were plotted versus inverse temperature as shown in figure 5.4. There is an obvious curvature apparent in the plots which is often observed for amorphous materials. In ionically conducting viscous liquids, such behavior is generally governed by the VTF equation[10]:

$$\sigma = A' \exp\{-[E_a/k(T-T_o)]\}$$

where E_a is the activation energy. This was, therefore, the first fit of the data attempted. Polymers, however, seem to better fit the VTF equation in the form:

$$\sigma = AT^{-1/2} \exp\{-[E_a/k(T-T_o)]\}$$

A nonlinear least squares fit was utilized to fit both forms of the VTF equation which yielded the results presented in table II for the best-fit parameters A', E_a, and T_o and A, E_a, and T_o.

The conductivities from the isothermal runs were also plotted, $\log_{10}\sigma$ versus pressure (see figure 5.5). The equation used to fit the resulting curves was:

---

[10] H. Vogel, Physik Z., 22, 645 (1921); V.G. Tammon & W. Hesse, Z. Anorg. Allg. Chem., 156, 245 (1926); G.S. Fulcher, J. Am. Ceram. Soc., 8, 339 (1925).

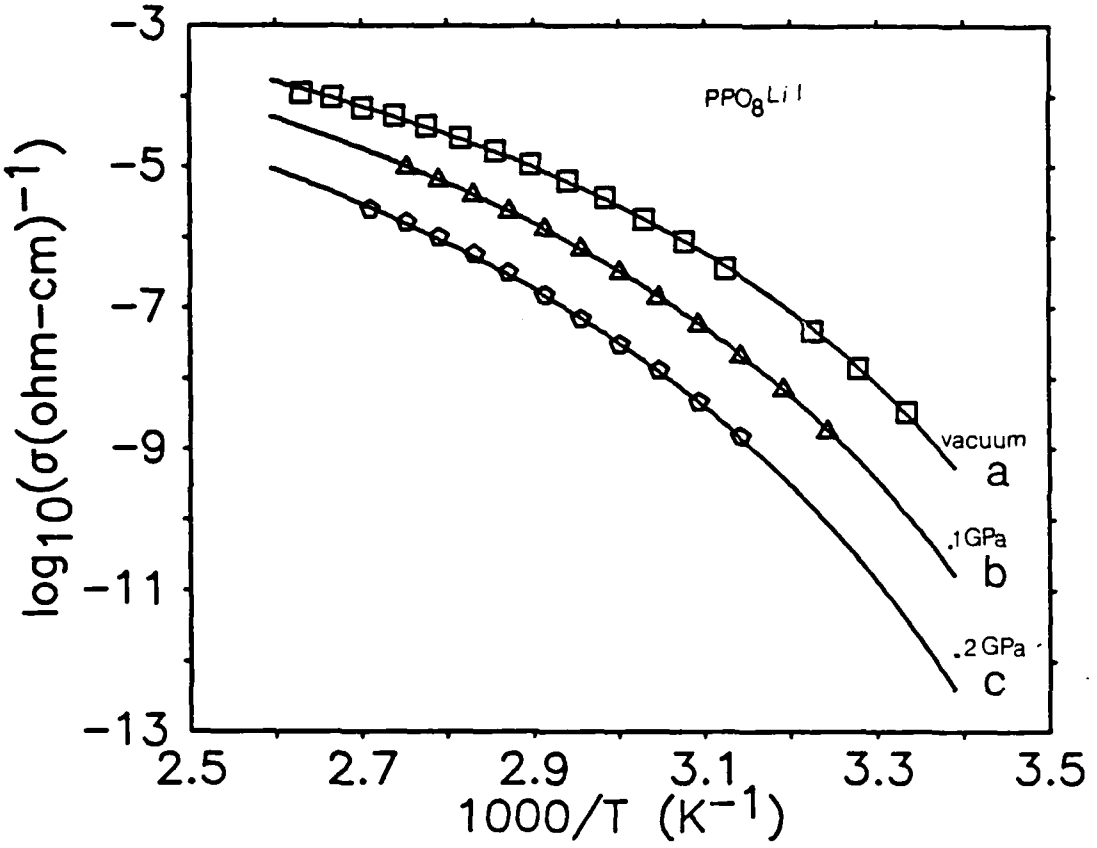

Figure 5.4 Isobaric conductivities.

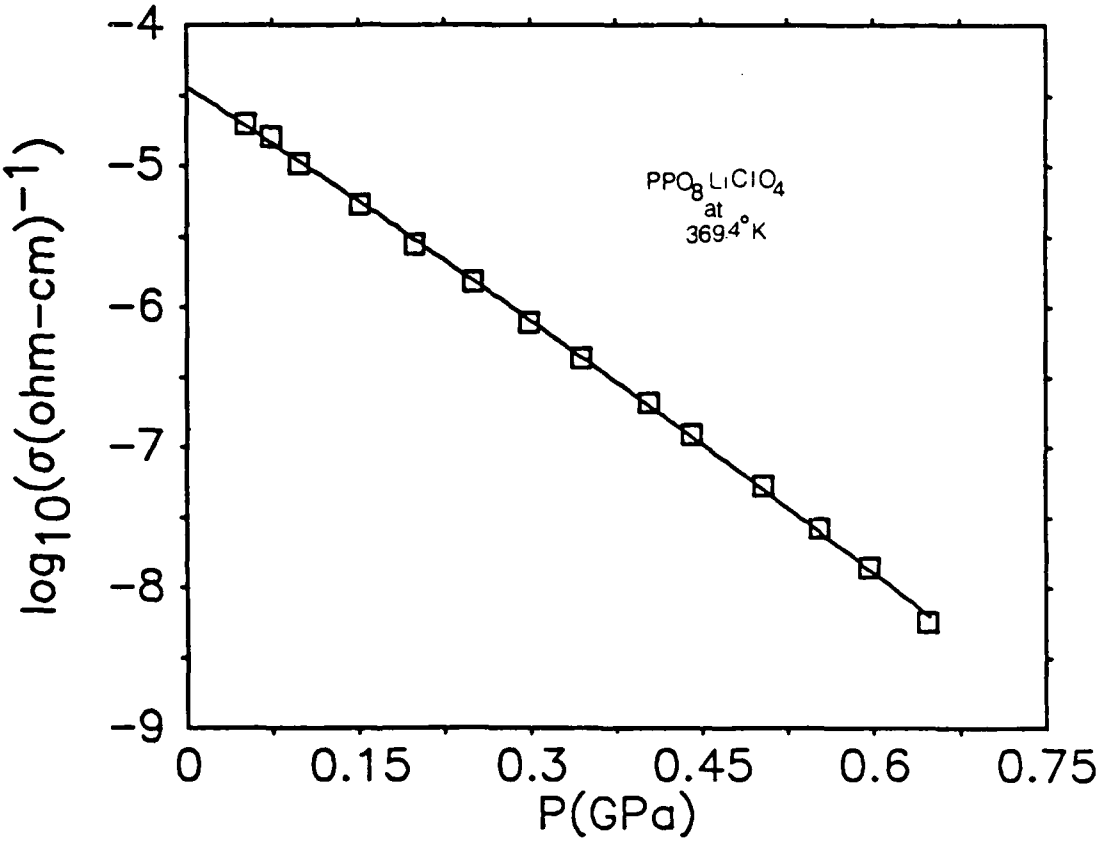

Figure 5.5 Isothermal conductivities.

$$\log_{10}\sigma = \log_{10}\sigma_o + aP + bP^2$$

Table III lists the best-fit parameters obtained. These plots were used to find 0.1 and 0.2 GPa (these are the pressures used on two isobaric runs) values of conductivity for comparison with the isobaric runs.

5.3b Analysis: Activation Volume. Since the activation volume is related to the pressure of the sample, the isothermal runs were further utilized to find the activation volumes for the salt complexed polymer samples. They were computed using the relationship:

$$V^* = -kT\, d\ln\sigma/dP$$

The results are listed in table III alongside the fitting parameters.

5.3c Analysis: Electrical Relaxation. The effects of pressure and temperature upon the α relaxation associated with the glass transition were also examined in pure PPO. Plotting the conductance per frequency versus the natural logarithm of frequency obtained from complex impedance analysis in vacuum, definite peaks are apparent (see figure 5.6). The peaks indicate the frequency of the α relaxation, and were positioned by fitting the imaginary part of the

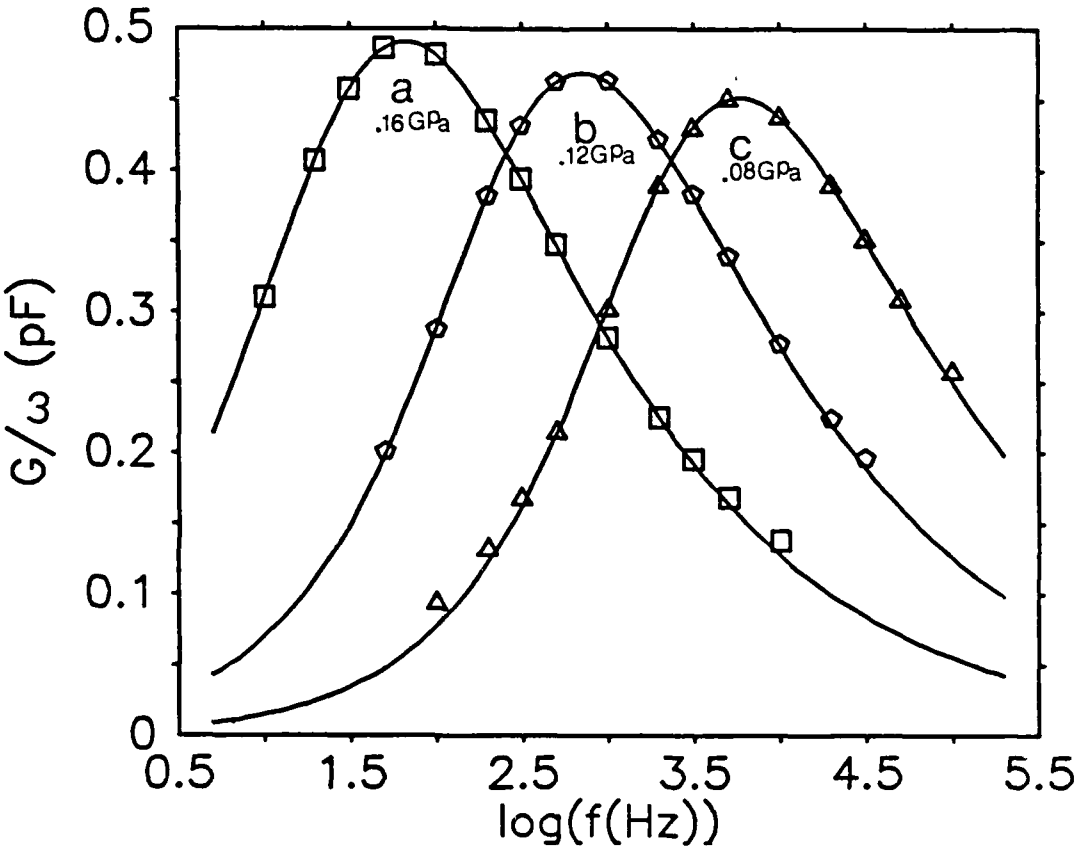

Figure 5.6 Relaxation peaks for PPO.

Havriliak-Nagami function[11]:

$$C^* = D[1 + (i\omega\tau_o)^{1-\alpha}]^{-\beta}$$

to the data yielding values for the parameters D, β, τ_o, and α.

Plots of the base ten log of these peak frequencies versus pressure and inverse temperature are shown in figures 5.7 and 5.8. They show obvious curvature similar to that exhibited by the conductivity plots. For this reason they were fit by analogous equations:

$$\tau = AT^{-1/2}\exp-[E_a/k(T-T_o)]$$

for the isobaric data and:

$$\log_{10}\tau = \log_{10}\tau_o + aP + bP^2$$

for the isothermal data. The zero pressure activation volumes were also computed from:

$$V^* = -kT\ d\ln\tau/dP$$

---

[11] S. Havriliak and S. Nagami, J. Polymer Science, C14, 99 (1966).

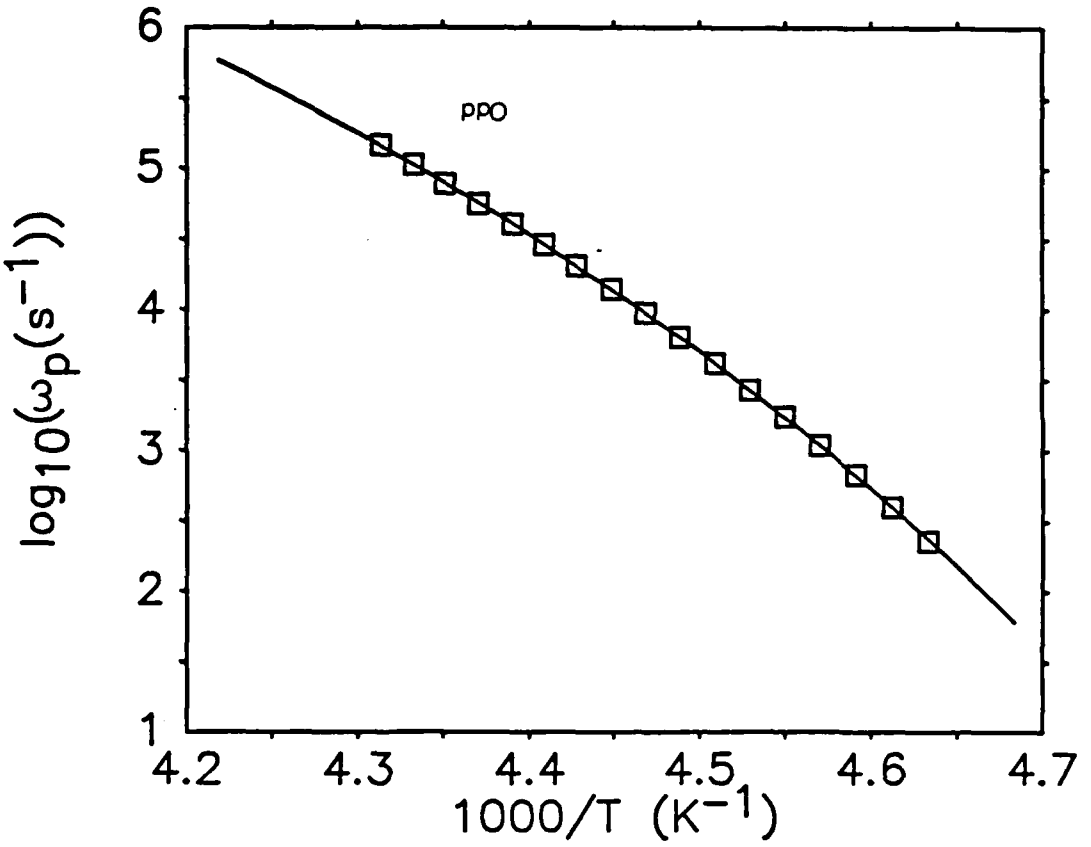

Figure 5.7 Relaxation time versus temperature.

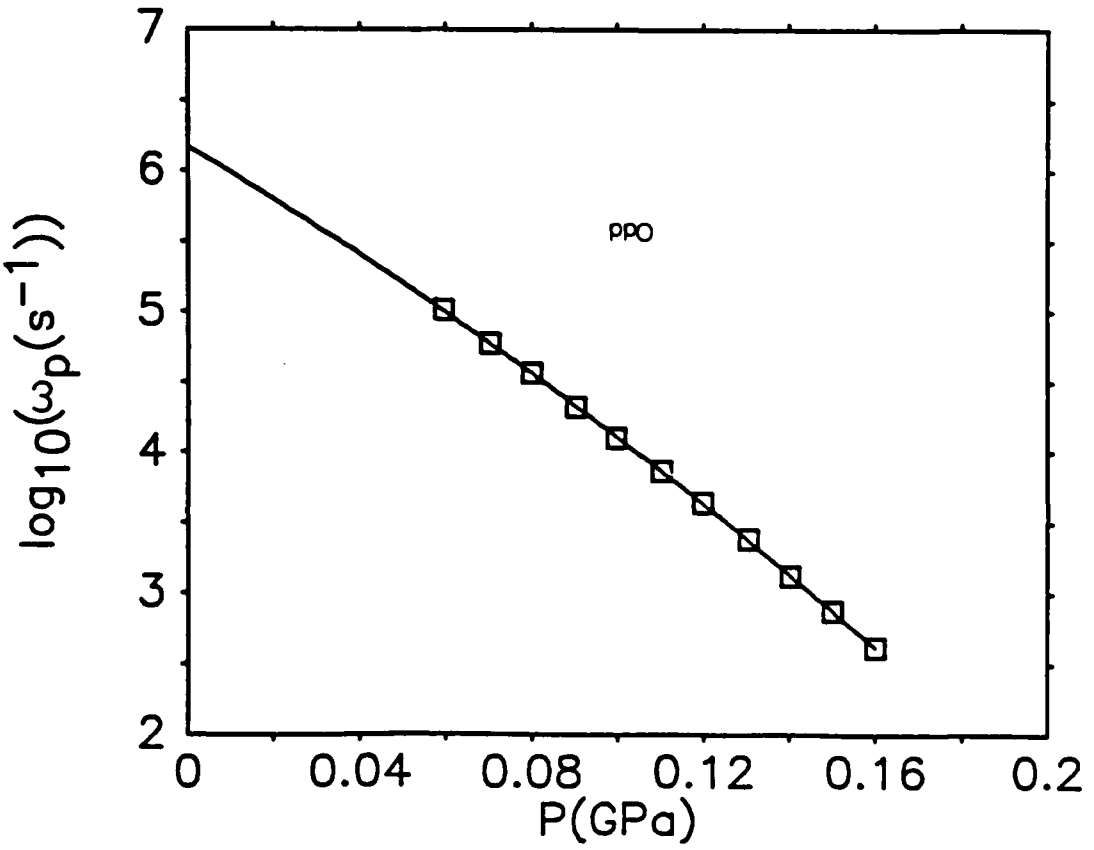

Figure 5.8 Relaxation time versus pressure.

The resulting values for the fitting parameters are displayed along with the appropriate conductivity results.

5.3d Analysis: Ion-implantation. The samples which were ion implanted were measured in the same apparatus as the chemically complexed samples. Because of time constraints, only one vacuum run was made for each implanted sample. These preliminary results produced two important results. First, the conductivity of the hydrogen-implanted samples showed no substantial increase in conductivity. The very-low-energy lithium-implanted sample, on the other hand, increased the conductivity of the PPO considerably.

6. Conclusions

There are a number of interesting yet obvious trends evident in the results of this research. The DSC results indicate the first of these trends, namely the shifting of the glass transition with the addition of salts into the polymer. Each of the four lithium salts added produced this effect. Notice, however, that while the shifted T_g's (middle) for the triflate and thiocyanate complexed samples differed by a significant amount, that of the perchlorate and iodide doped polymers are very similar. Moreover, this common value is the highest glass transition temperature present, indicating that it may be a limiting value for the transition temperature. It is also interesting to note that this shift results from the addition of the non-dipolar anions. This may result from the presence of anions with negligible interactions with polymer chains, and which by their presence, inhibit the motion characteristic of the chains in the rubber state.

For the PPO complexed with lithium triflate, there is an observed increase of T_o with pressure of about 10 K/kbar. Although this value is smaller than the 17 K/kbar change in T_g for the α relaxation in pure PPO, it appears to be somehow related. This pressure dependence of T_o is not observed for the samples prepared with the iodide and

perchlorate lithium salts. However, if Tg also does not exhibit a pressure dependence for these same materials, then a connection between To and Tg may still be argued. The strong shift of Tg by these substances may be evidence for a maximized shift of Tg which no further changes in pressure will alter.

It is also important to recognize the shifts in the activation energy with pressure for the complexed samples. Since it has be shown by Angell et al.[12] that all of the pressure dependence in liquids can be associated with the pressure dependence of To, this indicates that these ion conducting polymers cannot be modeled as viscous liquids.

Examining the activation volumes for the various samples is initially misleading if only the ion size is considered. In particular, the activation volumes increase from triflate to perchlorate to iodide while the anion size decreases in the same order. Therefore there can be no direct correlation between ion size and activation volume.

There is, however, a correlation between the activation volume and temperature relative to To. This can be seen quite plainly in a plot of V* versus the reduced temperature, T-To, as shown in figure 6.1. As the graph clearly indicates, the activation volumes for all the samples are

---

[12] C.A. Angell, L.J. Pollard, and W. Strauss, J. Solution Chemistry, 1, 517 (1972).

nearly equivalent for the same displacement from T_o. This simply means that the variations in activation volumes result from variations in T_o.

Although a relationship between T_o and V^* is obvious, the causal relationship between the two parameters is not as clear. One possible explanation is that both are intimately linked to the cationic transport number. This number is expected to be the greatest for the salts with dipolar anions, thiocyanate and triflate. Since these anions may be electrically attracted to and, thus interact with the polymer chains, fewer would be capable of moving freely within the material and a larger portion of the ionic current would be carried by the cations. Furthermore, by interacting with the polymer chains, these polar anions cause the dissociation of the salts thereby freeing up more lithium cations. The end result: a higher cationic conduction current.

A comparison of the results of fitting the theoretical expressions to the α relaxation data with that obtained from conductivity measurements reveals a good degree of agreement. The vacuum values of E_a from the conductivities is very close to that obtained from the α relaxation of pure PPO (with the exception of PPO_8:LiSCN[13])[14]. It is also

---

[13] The data from the thiocyanate doped polymer is suspected to contain water contamination.

apparent that T_o is about 50° below T_g for both the pure and the complexed samples. Finally, the activation volumes computed from the relaxation data are similar to those from the conductivity to within the normal spread of data. These correlations offer the first direct numerical evidence of a relationship between the mechanism involved in the α relaxation and that in the conductivity of the polymers tested.

The relationship between the activation volume and T_o as well as between the glass transition and T_o tend to support the configurational entropy model of ion conduction. In this model, T_o is interpreted as the temperature of minimum configurational entropy. The fact that it seems to control the activation volume necessary for ion conduction establishes its importance in this respect, while its correlation with T_g maintains its connection with the large-scale segmental motions characteristic with the glass-rubber transition.

The link between chain mobility and ionic currents was first proposed by Barker for PEO[15] ten years ago. The fact that these segmental motions may also control the degree of dissociation of the added salts could mean that they are

---

[14] From the results obtained it seems possible that the LiSCN may have been water contaminated.

[15] R.E. Barker, Jr., Pure & Appl. Chem., 46, 157 (1976).

linked only to the conductivity rather than the conduction mechanism per se. Further studies of ion implanted samples would help to clarify the role of these segmental motions in the conduction of ions as no dissociation of anions from cations is required in these doped materials. The development of a reasonable technique for cation implantation into polymer samples and the indication that direct cation implantation may alter the conductivity of the polymers accomplished in this research makes this a rather promising proposition for future study.

The research conducted for this study seems to indicate that an understanding of the mechanisms involved in ion conduction in polymers is approaching. At the present time, the role of a solid electrolyte seems best filled by amorphous polymers doped with lithium-salts containing polar anions.

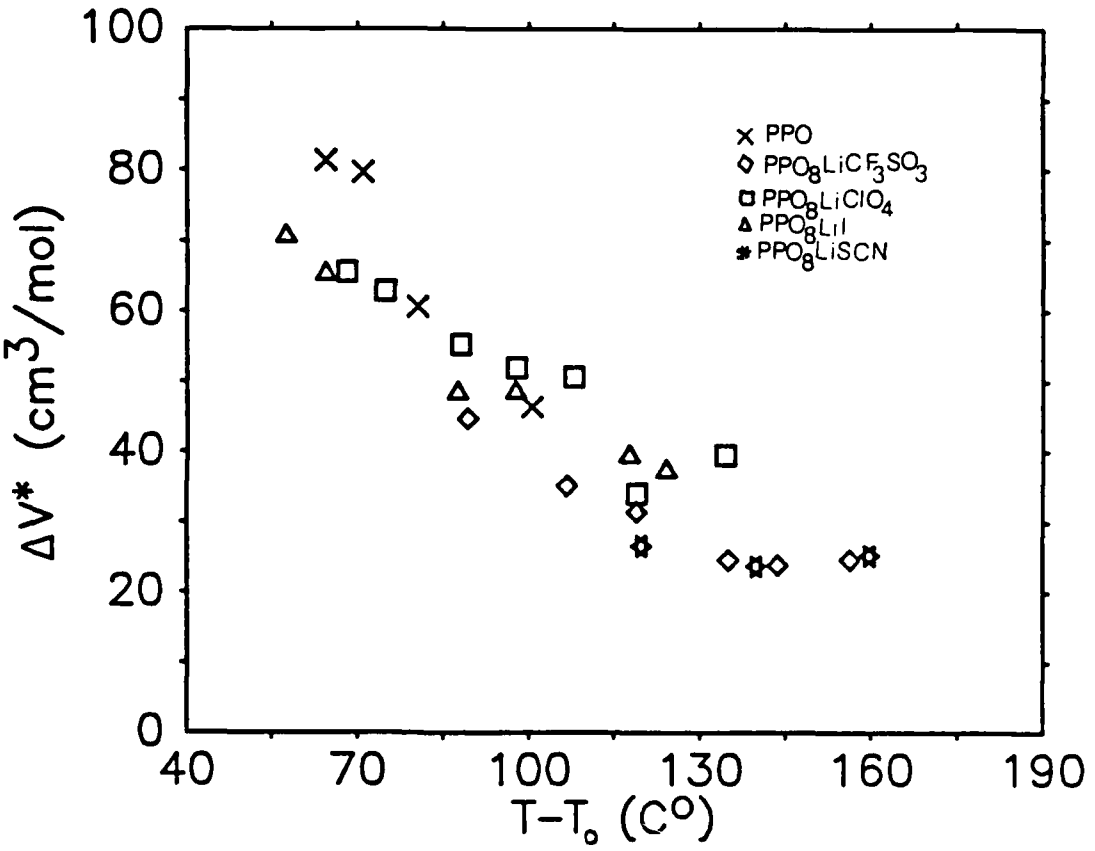

Figure 6.1 Activation volume versus reduced temperature.

Table I DSC results and best fit WLF parameters.

		T_g(K)	C_1	C_2(K)	$\log_{10}\sigma(T_g)(\Omega\text{-cm})^{-1}$ [$\log_{10}\omega_p(T_g)(s^{-1})$]	RMS Deviation
Electrical Relaxation (α)						
Uncomplexed PPO	Onset	208	12.6	35.3	[0.089]	0.0038
	Central	211	11.6	38.3	[1.076]	0.0038
	End	215	10.5	42.3	[2.174]	0.0038
Electrical Conductivity						
$PPO_8LiCF_3SO_3$	Onset[a]	238	18.7	22.0	-21.0	0.0146
	Central	248	12.9	32.0	-15.2	0.0146
	End	258	9.8	42.0	-12.1	0.0146
PPO_8LiClO_4	Onset[a]	263	14.8	26.4	-16.2	0.0111
	Central	281	8.8	44.4	-10.2	0.0111
	End	299	6.2	62.4	-7.7	0.0111
PPO_8LiI	Onset	268	18.9	21.9	-19.7	0.0233
	Central	283	11.2	36.9	-12.0	0.0233
	End	298	7.96	51.9	-8.76	0.0233
PPO_8LiSCN	Onset[a]	245	15.2	39.9	-16.1	0.0087
	Central	266	9.94	60.9	-10.9	0.0087
	End	285	7.58	79.9	-8.53	0.0087

Table II Best fit VTF parameters.

	RMS Deviation	$\log_{10}A$ $(\Omega\text{-cm})^{-1}\text{-}\sqrt{K}$ $[s^{-1}\text{-}\sqrt{K}]$	E_a(eV)	T_o(K)	RMS Deviation	$\log_{10}A'$ $(\Omega\text{-cm})^{-1}$ $[s^{-1}]$	E'_a(eV)	T'_o(K)
Uncomplexed PPO, electrical relaxation (α)								
Vacuum	0.0038	[13.95]	0.089	172.5	0.0038	[12.68]	0.088	172.7
$PPO_8LiCF_3SO_3$, electrical conductivity								
Vacuum[a]	0.0143	-0.94	0.086	214.0	0.0146	-2.34	0.082	216.0
0.1 GPa[a]	0.0054	-1.02	0.098	216.2	0.0055	-2.42	0.093	217.9
0.1 GPa[b]	0.0145	-1.06	0.086	226.2	0.0148	-2.45	0.082	227.6
0.2 GPa[a]	0.0142	-0.73	0.104	232.9	0.0143	-2.11	0.101	233.9
0.2 GPa[b]	0.0242	-1.03	0.092	233.6	0.0244	-2.41	0.089	234.6
PPO_8LiCLO_4, electrical conductivity								
Vacuum[a]	0.0110	-0.04	0.082	234.9	0.0111	-1.44	0.077	236.6
0.1 GPa[b]	0.0170	+1.11	0.094	236.4	0.0172	-0.26	0.091	237.4
0.1 GPa[b]	0.0435	+0.44	0.112	230.3	0.0436	-0.94	0.108	231.3
0.2 GPa[b]	0.0196	+1.03	0.103	242.6	0.0197	-0.34	0.100	243.3
0.2 GPa[b]	0.0692	+0.63	0.128	234.2	0.0692	-0.75	0.125	234.9
PPO_8LiI, electrical conductivity								
Vacuum	0.0226	+0.56	0.085	245.3	0.0233	-0.80	0.082	246.1
0.1 GPa[b]	0.0113	+0.97	0.114	240.3	0.0113	-0.40	0.111	241.0
0.1 GPa[b]	0.0304	+0.75	0.104	244.4	0.0303	-0.62	0.101	245.1
0.2 GPa[b]	0.0181	+0.72	0.127	241.1	0.0182	-0.66	0.124	241.8
0.2 GPa[b]	0.0822	+1.02	0.126	244.2	0.0820	-0.35	0.123	244.8
PPO_8LiSCN, electrical conductivity								
Vacuum[a]	0.0086	+0.047	0.126	203.2	0.0087	-0.95	0.120	205.1

Table III Best fit parameters and activation volume for isothermal data.

	T(K)	RMS Deviation	$\log_{10}\sigma_o(\Omega\text{-cm})^{-1}$ [$\log_{10}\omega_p(s^{-1})$]	$a(GPa)^{-1}$	$b(GPa)^{-2}$	ΔV^* (cm^3/mol)
Electrical Relaxation (α)						
Uncomplexed PPO	237.1	0.0055	[6.176]	-17.94	-26.5	81.4
	243.6	0.0071	[6.550]	-17.11	-21.3	79.8
	253.1	0.0079	[7.121]	-12.51	-18.4	60.7
	273.1	0.0063	[8.186]	-8.88	-8.49	46.4
Electrical Conductivity						
$PPO_8LiCF_3SO_3$	303.4	0.0181	-7.055	-7.72	-8.61	44.8
	320.8	0.0069	-6.272	-5.74	-5.34	35.3
	333.2	0.0138	-5.856	-4.95	-3.72	31.6
	349.1	0.0307	-5.436	-3.69	-3.16	24.7
	357.8	0.0241	-5.244	-3.51	-2.16	24.0
	370.4	0.0064	-5.008	-3.49	-1.11	24.7
PPO_8LiClO_4	303.0	0.0051	-7.303	-11.32	-11.80	65.7
	309.8	0.0172	-6.753	-10.60	-6.58	62.9
	323.1	0.0076	-5.938	-8.95	-5.25	55.4
	332.9	0.0139	-5.480	-8.15	-1.99	52.0
	343.1	0.0182	-5.093	-7.72	-0.37	50.7
	354.0	0.0822	-4.753	-5.03	-3.53	34.1
	369.4	0.0397	-4.370	-5.60	-0.42	39.6
PPO_8LiI	302.9	0.0070	-8.078	-12.20	-13.52	70.8
	309.9	0.0136	-7.281	-11.05	-9.46	65.5
	332.9	0.0026	-5.562	-7.61	-5.13	48.5
	343.1	0.0063	-5.061	-7.41	-7.07	48.7
	363.1	0.0193	-4.334	-5.70	-3.14	39.6
	369.4	0.0285	-4.156	-5.31	-1.76	37.5
PPO_8LiSCN[a]	323.1	0.0385	-6.081	-4.34	-4.33	26.8
	343.1	0.0059	-5.337	-3.62	-2.43	23.8
	363.1	0.0068	-4.782	-3.66	-1.01	25.4

REFERENCES

(1) "Battery Gets A Soft Cell", Sunday Times, London, 11-12-83.

(2) W. Archer and R. Armstrong, Electrochemistry, 7, 157 (1980).

(3) B. Papke, M. Ratner, and D. Shriver, Journal of the Electrochemistry Society, 192, 1694 (1982).

(4) L.C. Northcliffe and R.E. Schilling, Nuclear Data Tables, A7, 233 (1970).

(5) Paul F. Levy, "Thermal Analysis: An Overview", American Laboratory, January 1970.

(6) G.C. Kolodziejczak, Radiation Induced Dielectric Relaxation In Rare Earth Doped Calcium Fluoride, Report to the Trident Scholar Committee, Annapolis, MD: U.S. Naval Academy, 1978.

(7) M. Armand, Solid State Ionics, 9 & 10, 745 (1983).

(8) H. Vogel, Physik Z., 22, 645 (1921); V.G. Tammon and W. Hesse, Z. Anorg. Allg. Chem., 156, 245 (1926); G.S. Fulcher, Journal of the American Ceramic Society, 8, 339 (1925).

(9) S. Havriliak and S. Nagami, Journal of Polymer Science, C14, 99 (1966).

(10) C.A. Angell, L.J. Pollard, and W. Strauss, Journal of Solution Chemistry, 1, 517 (1972).

(11) R.E. Barker, Jr., Pure and Applied Chemistry, 46, 157 (1976).

END

10-86

DTIC